iron, 45; aluminum, 8.5; silica, 6; chromium, 3; cobalt, 0.10; potassium, 0.02; calcium, 0.06; and magnesium, 2.

It should be noted that *S. acuminata* is the fourth hyperaccumulator of nickel [that is, after *Hybanthus austrocaledonicus*, *Homalium guillainii*, and *Psychotria douarrei* (*3*)] discovered in the same location. This area consists of dense humid forest over peridotitic humus-rich alluvia in the vicinity of the Rivière Bleue. It would therefore seem that, unlike the case of *Hybanthus floribundus* (*6*), accumulation of nickel is not a xerophytic adaptation.

Table 1 shows the nickel content of various organs of *S. acuminata*. The data are based on the analysis of three specimens (one from the Rivière Bleue area, one from the Tontouta area, and another from the Forêt Cachée).

The nickel content of leaves and of other organs is very high (~ 1 to 2 percent), although comparable with most other hyperaccumulators from New Caledonia. Of special significance, however, is the extremely high nickel content of the latex which has 11.20 percent nickel on a wet weight basis and 25.74 percent when the data are expressed on a dry weight basis. This nickel concentration is nearly five times higher than for any other part of any other species and is easily the highest nickel concentration ever reported for any other living material (see Table 1). The cobalt content of the latex (0.007 percent) is extremely low compared with that of nickel. Values for other elements (in percentages: iron, 0.06; chromium, 0.004; potassium, 0.15; sodium, 0.11; magnesium, 0.052; and calcium, 0.52) are also relatively low.

The extremely high nickel content of the latex of *S. acuminata* poses interesting problems in plant physiology, since nickel contents as high as this would be fatal for most phanerogams. Preliminary experiments in our laboratory have resulted in the isolation of a low-molecular-weight, water-soluble organic complex of nickel whose composition has not yet been determined.

T. JAFFRÉ
Laboratoire de Biologie Végétale, Center O.R.S.T.O.M. de Nouméa, New Caledonia

R. R. BROOKS
J. LEE
R. D. REEVES
Department of Chemistry, Biochemistry, and Biophysics, Massey University, Palmerston North, New Zealand

References

1. G. Minguzzi and O. Vergnano, *Atti Soc. Toscana Sci. Nat. Pisa Mem.* **55**, 49 (1948).
2. B. C. Severne and R. R. Brooks, *Planta* **103**, 91 (1972).
3. T. Jaffré and M. Schmid, *C. R. Acad. Sci. Ser. D* **278**, 1727 (1974).
4. R. R. Brooks, J. Lee, T. Jaffré, *J. Ecol.* **62**, 493 (1974).
5. R. R. Brooks, J. Lee, R. D. Reeves, T. Jaffré, in preparation.
6. B. C. Severne, "Botanical methods for mineral exploration in Western Australia," thesis, Massey University (1972).

19 January 1976; revised 22 March 1976

Subjective Measurement of High-Order Aberrations of the Eye

Abstract. *We used an apparatus similar to Tscherning's aberroscope, and analyzed subjects' drawings to obtain the wave aberration surfaces of 55 eyes. This analysis permitted a Taylor series representation of the wave aberrations to terms of the fourth order. The results revealed a wide variety in type and severity of high-order aberrations in which "cylindrical" aberrations were prominent and cases of classical spherical aberration were rare. We computed the monochromatic modulation transfer function curves for the range of observations. The overall findings suggest a more prominent role for monochromatic high-order aberrations in degrading the visual image than has hitherto been assumed.*

Ordinary refractive corrections embodied in prescription spectacles specify three parameters for each lens (neglecting prism), namely, the sphere, cylinder, and cylinder axis. High-order monochromatic aberrations of the eye, for example, spherical aberration and coma, are usually neither diagnosed nor treated despite the famous dictum of Helmholtz (*1*) that the aberrations of the eye are such as would not be tolerated in any good optical instrument. With regard to diagnosis, this situation is doubtless due to the great difficulty attending most methods of aberration measurement hitherto employed (*2*).

We have developed a new subjective method for measuring the monochromatic aberrations of the eye (Fig. 1). The method is similar to that used with Tscherning's aberroscope (*3*). The subject monocularly views a point source of monochromatic light through a crossed-cylinder lens and grid assembly, which is held in a trial frame with the subject's normal distance lenses. Due to the strong astigmatism induced by the crossed-cylinder lenses, the pattern of the grid at the pupil is reproduced as a shadow image on the subject's retina, rotated through 90°, reversed left to right, and distorted by the aberrations of the subject's eye as follows: with no aberrations, the grid at the pupil will be transformed into a perfectly square grid on the retina and perceived as such. If, however, we envision an aberrant wave front at the pupil deviating from a perfect sphere by a distance $W(x,y)$ at any point, x,y, then the corresponding point on the retina, x',y', will be displaced from its aberration-free location by the amounts $\Delta x'$ and $\Delta y'$ where

$$\Delta x' = F(dz/dy) \quad (1)$$

$$\Delta y' = F(dz/dx) \quad (2)$$

and F is the focal length of the eye (*4*).

Whereas conventional lens aberration theory is based on the assumption of rotational symmetry of the optical elements, we have chosen to describe the wave-front aberration by a Taylor series, which makes no assumptions about the symmetry of the elements. Thus we may describe the wave-front aberration, $W(x,y)$ in terms of its coordinates x and y with origin at the center of the pupil (*5*):

$$W(x,y) = A + Bx + Cy + Dx^2 + Exy + Fy^2 + Gx^3 + Hx^2y + Ixy^2 + Jy^3 + Kx^4 + Lx^3y + Mx^2y^2 + Nxy^3 + Oy^4 \ldots \quad (3)$$

In this series representation of the wave aberration surface the terms Bx and Cy correspond to the conventional horizontal and vertical prism terms in an ophthalmic prescription and the terms Dx^2, Exy, and Fy^2 are transforms of the ordinary sphere, cylinder, and axis. The high-order aberrations are embodied in the subsequent terms, which we have represented through the fourth order. Each of these nine high-order terms gives rise to a characteristic distortion of the grid pattern resulting either in curvature or nonparallelism of the lines of the pattern (*6*) (Fig. 1). Terms with coefficients G through J specify third-order (comalike) aberrations while terms with coefficients K through O represent fourth-order aberrations. Classical spherical aberration is represented by the three terms K, M, and O in the ratio of 1 : 2 : 1. The pattern that the subject sees may be regarded as a square grid distorted in a manner determined by the Taylor series of Eq. 3, for which coefficients G through O are to be determined.

Each subject was asked to draw the pattern as he or she saw it. The locations of the intersections in the drawings were then recorded, and the Taylor

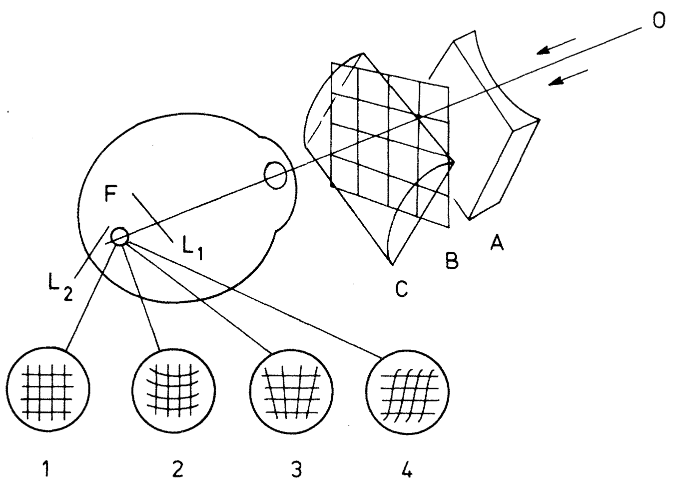

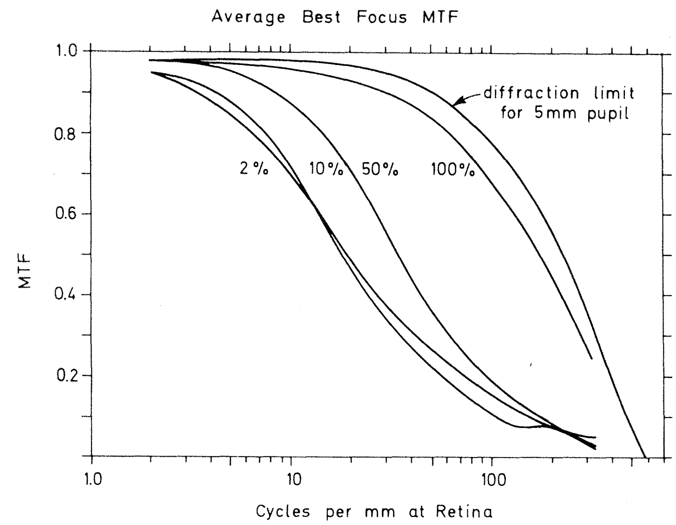

Fig. 1 (left). Formation of grid patterns on the retina. Collimated light parallel to axis traverses ±5 diopters crossed-cylinder lenses *A* and *C* with axes at ±45° and with an intercalated 1-mm² grid, *B*, and enters the pupil of the eye forming pattern at *F* on subject's retina. The two line foci, which define the interval of Sturm and arise from the induced astigmatism of the crossed-cylinder lenses, fall in front of and behind the retina at L_1 and L_2. Four possible patterns are envisioned for subjects with (1) no high-order aberrations, (2) with type *J* only, and (3) type *H* comalike aberrations, and (4) with type *K* fourth-order aberration. The crossed-cylinder lenses and grid compose a single compact test lens assembly, which is placed in a trial lens frame in front of the subject's prescription. Fig. 2 (right). Calculated monochromatic modulation transfer curves for 5-mm pupil diameter for selected eyes from a set of 55 rank-ordered eyes. The best eye is designated 100 percent. All curves were computed by the method of Hopkins (*10*). The ordinate is the average of horizontal and vertical meridian best-focus MTF's. The abscissa gives cycles per millimeter at the retina for a standard eye.

coefficients were determined by a computer program which fitted the *x* and *y* derivative surfaces of the wave aberration surface with two-dimensional orthogonal polynomials (*7*).

We studied 33 subjects and obtained useful drawings for 55 eyes, for which we computed the Taylor coefficients (*8*). The values of all the coefficients were then plotted as histograms, and their mean values and standard deviations were computed. The histograms for coefficients *G* and *I* were examined for any indication of nasal-temporal asymmetry such as would be due to coma caused by the known displacement of the optical axis relative to the axis of the eye; none was found. Similarly the *H* and *J* aberration distribution curves showed no effects attributable to gravimetric distortion of the eye.

By definition, the third-order aberration terms must dominate the aberration expression for sufficiently small pupil sizes. Using the total mean square wave-front deviation from a perfect spherocylindrical surface (*9*) as a criterion, we calculate that for a nearly physiological maximum pupil size of 8 mm, only 30 percent of our subjects' eyes were dominated by fourth-order aberrations; the rest were predominantly influenced by third-order aberrations. The result suggests that the classical view of the greater mischief of spherical aberration in degrading the visual image may be incorrect.

In classical spherical aberration the fourth-order terms *K* and *O* should have equal values in any given eye. In examining these coefficients, we found that few eyes exhibited appreciable classical spherical aberration, while approximately 20 percent of the eyes showed considerable amounts of either *K* or *O* aberrations singly. We have termed this condition "cylindrical aberration," that is, the aberration exhibited by a strong cylinder lens.

The combined effect of all Taylor aberration terms on degrading vision is perhaps best shown by the modulation transfer function (MTF). A pupil diameter corresponding to low light levels (5 mm) was chosen, and the 55 eyes were ordered by ranks according to the total mean square wave-front deviation from a perfect spherocylinder for this pupil size. The Taylor coefficients of eyes at selected rank-order percentile points were then used to compute by complex integration the best-focus vertical and horizontal MTF curves (*10*) (Fig. 2).

Drawing errors probably cause larger rather than smaller aberration coefficients, and, therefore, the actual visual performance of these selected eyes will probably be better than indicated. Despite this fact, we present the data because (i) they represent a fivefold larger population than has hitherto been studied (*11*), and (ii) the difference between our 50th percentile MTF and the theoretical estimates of van Meeteren (*12*) and others is sufficient, we believe, to warrant a reexamination of the significance of high-order aberrations in degrading vision (*13*).

Finally, we hope that this new, crossed-cylinder method of measuring aberrations, which was initially applied to the testing of camera lenses (*14*), will find useful application in clinical work. Because of its simplicity, we think that it could be used routinely in the diagnosis of irregular astigmatism, in following aberration changes in cases of suspected conical cornea, after corneal surgery, and for measuring the effects on high-order aberration of contact lenses.

BRADFORD HOWLAND
Research Laboratory of Electronics, Massachusetts Institute of Technology, Cambridge 02139

HOWARD C. HOWLAND
Section of Neurobiology and Behavior, Cornell University, Ithaca, New York

References and Notes

1. H. von Helmholtz, *Popular Lectures on Scientific Subjects* (Appleton, New York, 1885).
2. M. S. Smirnov, *Biophysics* **6**, 52 (1961). His method required 1 to 2 hours of measurement and 10 to 20 hours of computing per eye.
3. *Z. Psychol. Physiol. Sinnesorg.* **6**, 456 (1894).
4. The $+x'$ coordinate axis is defined as being to the subject's left; + values of y' are down (that is, maxillary) in accordance with the 180° rotation of images on the retina. The spacing of the undistorted grid at the retina will be $N\epsilon F$, where N is the dioptric power of the crossed-cylinder lens, ϵ is the actual grid spacing, and F is the focal length of the eye.
5. The coordinate system of the wave aberration surface has the $+z$ axis pointed inward along the foveal-pupil axis, the $+y$ axis pointed upward and the $+x$ axis pointing to the subject's right. A similar expansion for the wave-front aberration may be found in R. Barakat and A. Houston, *Opt. Acta* **13**, 1 (1966).
6. In this respect the method of this report differs significantly from that of Tscherning; with his method, finite values of four of the nine terms of the aberration function—*G, J, K,* and *O*—cause changes only in the spacing of the elements of the grid, whereas with our method these same terms result in either curvature or tilts. More-

over, with the new method, the pattern of the grid on the retina is sharper, since diffraction blurs the image of the lines along their length rather than their width.
7. For this purpose we construct two sets of polynomials that are orthogonal over the two (four- and five-line) integral sampling grids. We find a least-squares fit for the two derivative surfaces given by the x and y coordinate locations of the grid intersections of the subject's drawings and correct the derived coefficients for displacements of the axes of the grid relative to the center of the pupil.
8. Our subjects included approximately equal numbers of males and females with an average age of 25 ± 8 (standard deviation) years and no obvious visual pathology.
9. Circular, orthogonal Zerninke polynomials were computed from our measured Taylor coefficients [M. Born and E. Wolf, *Principles of Optics* (Pergamon, Oxford, ed. 5, 1975)]. The root-mean-square deviation of the wave aberration surface from a perfect spherocylinder (computed from the Zerninke coefficients) is useful in the image evaluation of small aberrations. Here it is convenient for ordering the nine-dimensional high-order aberration wave surfaces according to severity.
10. H. H. Hopkins, *Proc. Phys. Soc.* **79**, 889 (1962).
11. Smirnov (2) published topographic diagrams of the wavefront aberration surfaces for 12 eyes. See also the measurement of the MTF of one eye by F. W. Campbell and D. G. Green [*J. Physiol.* **181**, 576 (1965)].
12. A. van Meeteren, *Opt. Acta* **21**, 395 (1974).
13. Two additional ways of obtaining the aberration coefficients are with (i) computer generation of a distorted pattern, which the subject compares with the perceived pattern with the aid of a camera lucida, and (ii) an electronic aberration synthesizer that allows the subject to adjust the apparatus so that he perceives a perfectly square grid, thus nullifying his own aberrations.
14. B. Howland, *Appl. Opt.* **7**, 1587 (1968).
15. During the period of this research, B.H. was a staff member of the Massachusetts Institute of Technology Lincoln Laboratory, Lexington, and a research affiliate in the Research Laboratory of Electronics, Massachusetts Institute of Technology, with support from NIH grant 5 R01 EY 01149, and by a grant from Bell Telephone Laboratories, Inc. A preliminary report of this work was presented at the spring 1974 meeting of the Optical Society of America [*J. Opt. Soc. Am.* **64**, 554 (1974)]. We thank our subjects and undergraduate research assistants, D. Daly, C. Miller, R. Redberg, J. Klopfer, S. Lipkowitz, M. Bielman, and J. Mayberry; we also thank M. Howland for drafting assistance, Drs. J. Sivak and A. van Meeteren for reading an earlier version of this manuscript, and Dr. J. Y. Lettvin for advice and encouragement.

10 February 1976

Transplanted Neural Tissue Develops Connections with Host Rat Brain

Abstract. *Superior collicular fragments transplanted from fetal to newborn rat brains develop complex internal organization and receive visual afferents from the host providing they lie sufficiently close to the host visual pathways. This system allows investigation in vivo of special affinities between cells of the mammalian central nervous system.*

The vertebrate nervous system exhibits predictable patterns of interconnections that persist when cut axons regenerate in vivo (*1*) and, in some cases, even when neuronal tissues are cultivated in vitro (*2*). To explain the origin of this predictability, Sperry (*3*) proposed that neurons acquire unique cytochemical labels whose selective matching leads to the formation of ordered connections between different brain regions. This general hypothesis is supported by cell aggregation experiments that demonstrate region-specific affinities between neuronal cells (*4*), but these studies are still several steps removed from explaining the development of ordered synaptic connections. Furthermore, the interpretation of any in vitro experiment is clouded by the observation that neurons are capable of substantial modification and reorganization of connections. For example, in fish, amphibia, and developing mammals, removal of afferents to certain regions often causes major reorganization of other inputs such that they invade and form functional synapses in the deprived region; conversely, removal of the target area of a growing axon population may cause these axons to innervate adjacent regions (*5, 6*). At the level of individual neurons, such results suggest that identifying cytochemical labels are not irreversibly determined, or that factors other than special affinities between axons and their postsynaptic cells play a role in the development of ordered neuronal connections.

The present study demonstrates a way in which these problems may be systematically investigated in the developing mammalian nervous system and addresses the specific question of whether neuronal populations are automatically innervated by a group of axons if placed in the terminal field of those axons. The approach entails transplantation of tissue fragments from the superior colliculus of fetal rats into the superior colliculus region of newborn rats and the subsequent demonstration of synaptic connections between host and transplanted tissues. Two features make this feasible: (i) afferent pathways to the superior colliculus of rats are still capable of growth through lesions or of modified growth in response to specific surgical manipulation at birth (*5*); and (ii) newborn rats have not developed immunological competence and so will not reject the transplants (*7*). A similar approach involving transplantation of regions of fetal rat brain into the cerebellum of rats after birth was reported by Das (*8*) but, while demonstrating transplant survival, he did not investigate the formation of connections between transplant and host in that study.

Pregnant rats were injected with [^{3}H]thymidine on fetal day 13 or 14, the days when terminal cell division in the colliculus is most frequent. On day 15 or 16, fetuses were removed and the tectum separated from the rest of the brain in

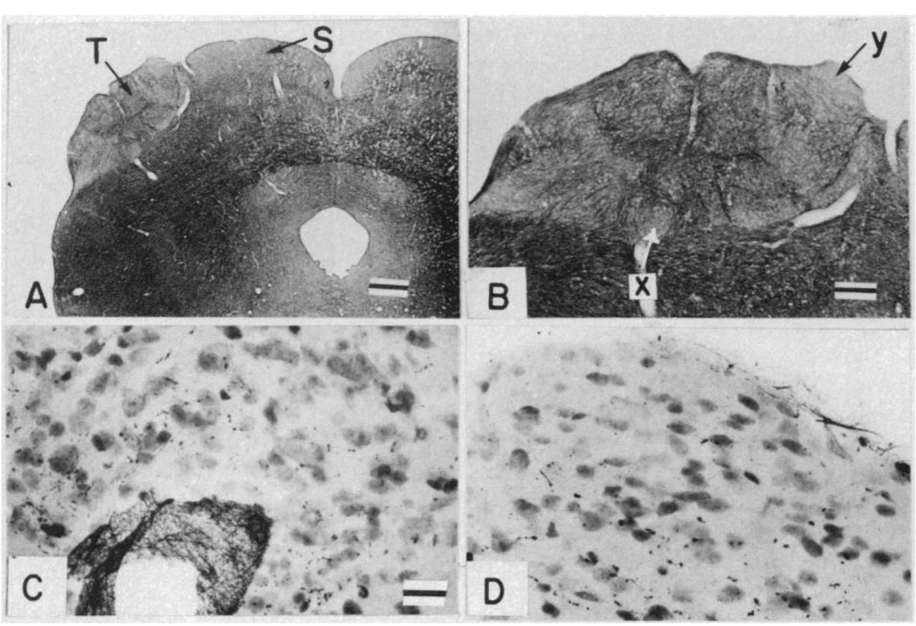

Fig. 1. (A) Transverse section through midbrain showing transplant (*T*) in upper layers of host superior colliculus (*S*); neurofibrillar stain; scale bar, 450 μm. (B) Detail of transplant in (A). Adjacent Fink-stained sections show an optic projection to the two areas (*x* and *y*); scale bar, 200 μm. (C and D) Details from section adjacent to that in (A) and (B), stained by Fink-Heimer method and showing degenerating optic terminals in regions *x* and *y*, respectively. No other part of this transplant showed terminal degeneration; scale bar, 20 μm.